ELSEVIER

International Journal of Solids and Structures 41 (2004) 5301–5311

INTERNATIONAL JOURNAL OF SOLIDS and STRUCTURES

www.elsevier.com/locate/ijsolstr

Modeling of the monotonic and cyclic swift effects using anisotropic finite viscoplasticity theory based on overstress (AFVBO): Part I—Constitutive model

Ozgen U. Colak [1]

Mechanics of Materials Laboratory, Rensselaer Polytechnic Institute, Troy, New York 12180-3590, USA

Received 30 June 2003; received in revised form 23 February 2004
Available online 20 May 2004

Abstract

The isotropic finite viscoplasticity theory based on overstress (FVBO) is extended to anisotropy. It is accomplished by formulating an anisotropic flow law, which consists of a fourth order inelastic compliance tensor. Since large inelastic deformation causes a change in the microstructure, the aforementioned tensor is allowed to evolve according to the Frederick–Armstrong type law during inelastic deformation. Additive decomposition of the rate of deformation into elastic and inelastic parts is assumed. The current configuration is taken as a reference configuration.

Keywords: Anisotropy; Swift effect; Free-end torsion; Viscoplasticity

1. Introduction

Numerous finite deformation plasticity and viscoplasticity theories have been developed in the last decades to simulate complex forming processes such as rolling, wire drawing, sheet metal forming and extrusion. Forming processes introduce changes of the metallic material to be formed. Strength properties can change as well as directional properties. These complex, non-homogenous deformation and loading conditions make the constitutive model development difficult. Constitutive models need information from experiments that are performed in homogenous states of stress. Examples are: torsion and axial loading of a thin-walled tube.

One of the interesting phenomena in large torsion tests of thin-walled tubes is that depending upon test conditions, free-end torsion induces axial length changes whereas fixed end torsion results in an axial stress build up. These axial length changes known as the Swift effects are attributed to deformation induced anisotropy, see Montheillet et al. (1984), Neale et al. (1990) and Wu et al. (1998).

E-mail address: colako@alum.rpi.edu (O.U. Colak).

[1] Present Address: Yildiz Technical University, Istanbul, Turkey.

0020-7683/$ - see front matter
doi:10.1016/j.ijsolstr.2004.04.013

The first part of this paper consists of a review of experimental work. Monotonic and cyclic free and fixed end torsion experiments will be discussed. Correlation between axial length changes and anisotropy will be briefly given. The second part focuses on macroscopic modeling efforts. In the last section, the finite VBO is extended to deformation induced anisotropy. It is accomplished by introducing an inelastic compliance tensor and allowing it to evolve with large inelastic deformation.

2. Historical review of experimental data

The inelastic axial elongation in finite free-end torsion loading was first observed by Swift (1947) and is hence called the Swift Effect. Swift conducted free-end torsion tests on seven different metals: 70–30 brass, stainless steel, aluminum, cupro-nickel, copper, mild steel and 0.5% carbon steel at room temperature and observed the deformation for solid cylindrical bars. All seven materials elongated under torsional strain as shown in Fig. 7 of Swift (1947). The form of shear strain vs. axial strain curves changes for different materials and the shear strains in the order of 3 generate axial strains of 3% (carbon steel) and 11% (70:30 brass).

Swift (1947) also examined the effects of a reversal of torsion. Such tests were carried out on 70:30 brass, stainless steel, copper and mild steel. It was shown that upon reversing the direction of the shear strain at various shear strain levels, the magnitude of the axial strain was initially observed to decrease followed by an increase as shown in Fig. 1 which is reproduced from Majors and Krempl (1994) who in turn obtained the data from Fig. 10 of Swift (1947). Similar tests were performed with other materials. It was seen that the form of the unloading curve changes considerably from metal to metal. For example, in mild steel with prior tensile straining, the unloading curve follows the loading curve. Tests were also carried out on thin-walled tubular specimens to compare the results with those of the solid bar specimens. Thin-walled tubes were found to exhibit behavior very similar to the solid bar specimens.

To examine the effects of strain hardening, Swift (1947) also conducted torsion tests on lead bars, which exhibit softening at room temperature. Axial shortening of the bar occurred at large shear strain. It was concluded that strain hardening was the mechanism for the axial elongation of the other alloys.

The Swift effect, which is the elongation of a tubular or solid bar specimen under free-end torsion, is examined by Billington (1976, 1977a,b). Experiments were carried out on aluminum, copper, iron and aluminum alloy at room temperature. The copper was tested as annealed and "as-received" condition.

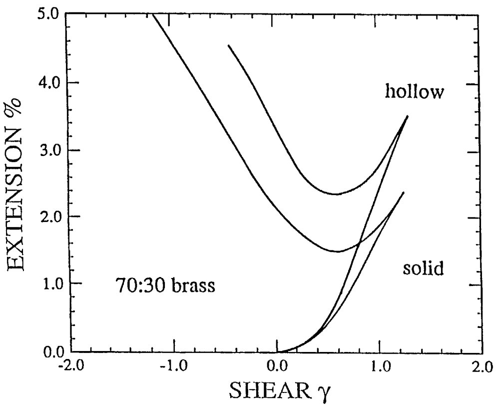

Fig. 1. Axial length change of hollow and solid brass specimen under free-end torsion. Reproduced by Majors and Krempl (1994) from Fig. 10 of Swift (1947).

Axial elongation similar to Swift's results is observed. Only one contradiction with Swift's experiments was observed in iron. Although the iron exhibits almost no hardening after 100% plastic shear strain, it elongates considerably. This result contradicts the Swift's conclusion about the relation between the length change of twisted tubular or solid specimens and work hardening. Considering the behavior of iron, it was concluded that work hardening was not the only mechanism for axial elongation as Swift stated.

Montheillet et al. (1984, 1985) examined the relation between axial stresses and texture development during fixed-end torsion test. Aluminum, copper and α-iron specimens were tested at temperatures between room and the hot working range. First, axial forces were measured. Then, the textures, which were developed during these tests, were determined. At low temperature, axial forces were compressive in all three materials. They decreased when temperature was increased. In the case of copper and α-iron, axial stresses became tensile. Pole figures, which show the rotations or tilting of texture from ideal orientations, were obtained using the X-ray diffraction method. It was observed that when magnitude and sign of axial forces changed, intensity and rotation of the ideal orientations were also changed. Thus, axial forces have their origin from the induced anisotropy of the mechanical properties of the material.

Wu et al. (1998) conducted a series of free and fixed end torsion experiments on cast and extruded high purity aluminum materials. The annealed cast aluminum was initially isotropic, while the annealed extruded aluminum had a texture which the grains are aligned along the extrusion direction. Experiments were performed at room and high temperature. The axial elongation developed during free-end torsion and compressive axial stresses developed during fixed end torsion. It is found that axial elongation was less for the cast aluminum than extruded aluminum which was anisotropic at the beginning of the experiment as shown in Fig. 11 of Wu et al. (1998). Experimental data obtained from Swift (1947), Billington (1976) and Wu et al. (1998) can be found in Table 1.

Table 1
Laboratory experiments

Author	Material	γ[a]	*El* (%)[b]	Reversal
Swift (1947)	70:30 Brass	4.5	11.5	At shear strain of 1.2
	Stainless steel	2.8	6.3	At shear strain of 1.3
	Aluminum	5.9	7.1	No
	Cupro-nickel	5.8	4.0	No
	Copper	4.5	3.6	At shear strain 1.3 and 2.5
	Mild-steel	3.0	3.5	At shear strain of 1.3
	0.5% Carbon steel	1.0	1.0	No
Billington (1976)[c]	Aluminum	1.0	2.0	No
	Copper	2.0	3.6	No
	Annealed copper at 550 °C	2.0	2.2	
	Iron	2.8	12.0	No
	Aluminum alloy	1.0	2.0	No
Wu et al. (1998)	Annealed cast aluminum	1.9	3.0	No
	Annealed extruded aluminum	1.5	6.0	No

[a] Maximum shear strain.
[b] Maximum axial strain.
[c] Maximum strain is plastic shear strain.

3. Texture development

Inelastic deformation usually results in changes of the internal structure of materials. These changes can be broadly classified into two categories, namely defect structure changes and orientational changes, (Lehmann, 1990). The former involves changes in the dislocation density through the generation and elimination of defects. It might also represent the migration and pile-up of dislocations at grain boundaries. The latter, orientational changes, involves the reorientation of grains along preferred directions to produce texture. These aligned grains give rise to anisotropy. As a result of the anisotropy, a common observation is the dependence of material properties, for instance Young modulus (E), on the direction.

4. Modeling efforts

There are few theories describing the anisotropic elastic and plastic deformation behavior of materials during large deformation. The approaches are microstructural or phenomenological. The former approach is followed by Asaro and Needleman (1985), Neale et al. (1990) and Taylor (1938). Lee and Zaverl (1978, 1979), Shih and Lee (1978), Lee (1978), Krempl (1994), Kuroda (1997), Van der Giessen et al. (1992), Voyiadjis and Kattan (1992) and Nouailhas and Chaboche (1991) employ a phenomenological approach for inelastic analyses. The crystal plasticity models, which are one of the microscopic approaches, are used to describe crystallographic texture and stress–strain behavior. Crystal plasticity models can be described using slip system concepts, see Taylor (1938), Asaro and Needleman (1985), Lowe and Lipkin (1991), Wu et al. (1996), Neale et al. (1990), Harren et al. (1989), Bertram et al. (1997). In these approaches, microstructural changes are used to describe macroscopic material behavior. Macroscopic models range from rate independent plasticity models to unified state variable theories. In this paper, we will focus on macroscopic models.

4.1. Rate independent plasticity models

Rate independent plasticity models have been used for the modeling of anisotropy. Analyses of axial effects, which are induced axial strain or stress during torsion have been performed by using kinematic hardening laws with plastic spin (e.g. Van der Giessen et al., 1992; Voyiadjis and Kattan, 1992). Kinematic hardening is considered as repository for anisotropy. Nevertheless, it is shown that kinematic hardening law is not enough to model anisotropy (Majors and Krempl, 1994). Inadequacy of kinematic hardening law for cyclic loading led to the development of anisotropic yield surfaces and models which contains anisotropic flow law, see Hill (1953), Mroz and Niemunis (1990), Majors and Krempl (1994) and Gomaa (1999).

4.1.1. Modeling of anisotropy with isotropic yield surface

The behavior of materials under free and fixed-end torsion has been investigated using isotropic yield surfaces. A kinematic hardening or combined isotropic and kinematic hardening law has been incorporated into von Mises yield criterion, see Van der Giessen et al. (1992) and Voyiadjis and Kattan (1992), to analyze torsion behavior of the materials.

Van der Giessen et al. (1992) used a combined isotropic–kinematic hardening model with two different plastic spins to analyze the large strain behavior of solid circular bars under torsional loading conditions. They focused on the effect of plastic spin on axial elongation and axial stress. The isotropic von Mises yield surface with two combined isotropic–kinematic hardening laws is used. Hardening models considered are the kinematic hardening model proposed by Dafalias (1990) and Loret (1983) (DL model) and Van der Giessen et al. (1992) (VDG model). The DL model uses an associated flow rule and the plastic spin, $\mathbf{W}^{p}$ is defined by

$$W^{\mathrm{p}} = \frac{\lambda}{2}\bar{\rho}(\mathbf{a}\bar{\mathbf{s}} - \bar{\mathbf{s}}\mathbf{a}) \quad (1)$$

where λ and $\bar{\rho}$ are material parameters, $\mathbf{a}$ is back stress which is considered as representation of induced inelastic anisotropy and $\bar{\mathbf{s}}$ is the difference between deviatoric Cauchy stress and back stress. The evolution equation for the back stress is taken as a Prager–Ziegler type rule, which defines the back stress as a function of inelastic rate of deformation. In VDG model, plastic spin is determined by the skew part of back stress, specifying the translation of the yield surface. The velocity gradient tensor is used for obtaining the objective rate of the back stress. Simulations were performed only for monotonic torsion loading. It is shown that plastic spin has an important effect on the axial strain development during free and fixed end torsion and DL models tend to give smaller axial strain than the VDG model.

Similar to the work of Van der Giessen et al. (1992), Voyiadjis and Kattan (1992) analyzed the torsion with free and fixed end boundary conditions by using a von Mises type yield criterion. Three different spins are used and their effects were investigated under monotonic loading condition. The plastic spins used in the simulations are:

(1) The plastic spin defined by Dafalias (1990) given in Eq. (1).
(2) The plastic spin is defined as $\mathbf{\Omega} = \omega\mathbf{W}$ where $\mathbf{\Omega}$ is a skew symmetric spin tensor and $\mathbf{W}$ is the skew part of the velocity gradient tensor.
(3) When the quantity ω is taken to be a positive constant, decrease in the axial stretch with increasing shear strain is observed, see Fig. 14 of Voyiadjis and Kattan (1992). On the other hand, when ω is chosen as a function of back stress, oscillations in the axial stretch are observed, see their Fig. 15.

4.1.2. Modeling of anisotropy with anisotropic yield surface

Anisotropic yield criterion started to be developed by Hill (1953). He modified the Tresca or von Mises isotropic yield criterion to describe the yielding of anisotropic materials. The following assumptions were made: the material is orthotropic, hydrostatic stress does not effect the yielding and there is no Bauschinger effect.

Following Hill's anisotropic yield surface concept, two anisotropic surfaces are defined by Mroz and Niemunis (1990) to model the anisotropic behavior of the materials. These surfaces are called anisotropic texture surface and anisotropic yield surface respectively. There are two main reasons for anisotropy, one is related to preferred crystallographic structure in metals, the other is associated with back stress caused by plastic deformation. A fourth tensor, $\mathbb{A}$ called anisotropy tensor is incorporated into the anisotropic texture surface and is allowed to evolve during deformation as a function of inelastic strain. The same fourth order anisotropy tensor $\mathbb{A}$ is used in the evolution equation of yield surface. Tensor $\mathbb{A}$ is defined only for an orthotropic material. A change in the material symmetry, which can be observed during inelastic deformation, was ignored. Further investigations are needed to account for a change in the shape of the yield surfaces.

4.2. Viscoplasticity models

The second class of continuum theories contains viscoplasticity theories which assume that inelastic deformation is rate dependent even at low homologous temperatures. The development of viscoplasticity models was motivated by two main conclusions about classical plasticity models:

1. Plasticity models can be handled easily in numerical simulations and are being used in several commercial finite element codes. They predict the initial yield of materials quite well. Shape change of the yield surface is observed during finite non-proportional multiaxial loading in addition to size and position

changes. The evolution of the shape change is, however, not easily quantified (Stouffer and Dame, 1996). New internal variables can be incorporated into the isotropic and kinematic hardening laws to define the non-circular yield surface (Khan and Cheng, 1998). In addition, experiments have shown that the plastic strain increment vector is not normal to the yield surface during non-proportional loading. Therefore, the applications of classical plasticity models are limited to proportional loading, see Stouffer and Dame (1996).
2. All time effects, such as rate sensitivity, creep, relaxation and strain recovery are excluded in the classical plasticity models. Experiments, however, exhibit rate dependency even at room temperature (Krempl, 1998).

The viscoplasticity models represented by unified state variable theories do not permit the separation of creep and plasticity. State variables are defined as macroscopic averages of events associated with microstructure changes (Stouffer and Dame, 1996), and cannot be directly measured or controlled, but they are useful in defining material behavior. These variables are associated with dislocations and their interaction with other dislocations and grain boundaries. One example of state variables can be given the back stress. Back stress is the resistance to slip, see Stouffer and Dame (1996). It results from the interaction of dislocations with other dislocations, grain boundaries and other barriers. It is introduced in state variable theories to model hardening and recovery effects associated with dislocation pile-ups.

4.2.1. Modeling of anisotropy with isotropic viscoplasticity models

A viscoplastic model with an isotropic flow rule and isotropic yield surface is used by Kuroda (1997) to model the cyclic Swift effect. Kinematic hardening is considered as the only repository of anisotropy. Contrary to experimental observation, see Fig. 1, after unloading, axial elongation does not track back but continues to grow.

All models considered by Majors and Krempl (1994) were classified into two categories: Class A and Class B. The former refers to the models which use the combination of an isotropic flow law and kinematic and isotropic hardening rule. The latter refers to the models, which use an anisotropic flow law. In the Class A model, the back stress is the repository for induced anisotropy. Majors and Krempl (1994) investigated the material behavior under free-end torsion using isotropic finite viscoplasticity theory based on overstress (VBO) which is also a Class A type model and contains an isotropic flow law and three state variables which are equilibrium stress, kinematic stress and isotropic stress. The evolution law for kinematic stress is chosen as a Frederick–Armstrong type model. They modified the plastic spin introduced by Dafalias (1990),

$$\mathbf{\Omega} = \mathbf{W}^{\mathrm{in}} - \mathbf{W}^{\mathrm{r}} \tag{2}$$

where $\mathbf{W}^{\mathrm{in}}$ is inelastic part of the spin tensor. $\mathbf{W}^{\mathrm{in}}$ can be approximated to the spin tensor $\mathbf{W}$. Dafalias (1990) initially used an antisymmetric tensor, $\mathbf{W}^{\mathrm{r}}$ which is given in Eq. (1). Majors and Krempl (1994) modified the Dafalias' plastic spin by replacing the Cauchy and back stress by kinematic stress, $\mathbf{K}$ and the inelastic rate of deformation tensor, $\mathbf{D}^{\mathrm{in}}$. Considerations behind these changes were: the kinematic stress and the inelastic rate of deformation tensor are two repositories for deformation induced anisotropy. Majors and Krempl (1994) defined $\mathbf{W}^{\mathrm{r}}$ as follows,

$$\mathbf{W}^{\mathrm{r}} = c(\mathbf{K}\mathbf{D}^{\mathrm{in}} - \mathbf{D}^{\mathrm{in}}\mathbf{K}) \tag{3}$$

where c is a material constant.

A particular material was not modeled quantitatively. While axial elongation is observed at monotonic torsion with Class A model, reversed free-end torsion behavior cannot be modeled. After unloading, axial elongation continues to grow, no backtracking is observed. It is concluded that Class A type models can model only the monotonic Swift effect and this type of models is not capable of modeling the reversed behavior during loading and unloading.

4.2.2. Modeling of anisotropy with anisotropic viscoplasticity models

Kuroda (1997) examined the behavior of the materials under large inelastic shear deformation. An anisotropic yield surface is introduced into the viscoplasticity model. The anisotropy is restricted to orthotropy for simplicity. For the first time, plastic spin, which is a function of the Cauchy stress and inelastic rate of deformation tensor, is coupled with an anisotropic flow law. The backtracking after the unloading can be reproduced successfully by this approach. The effects of spin were examined using continuum spin, which is equal to skew part of velocity gradient and the Euler spin. The Euler spin is defined by $\dot{\mathbf{Q}}\mathbf{Q}^{\mathrm{T}}$ where $\mathbf{Q}$ is the orthogonal tensor diagonalizing the left stretch tensor $\mathbf{V}$ as $\mathbf{V} = \mathbf{Q}\mathbf{\Lambda}\mathbf{Q}^{\mathrm{T}}$. $\mathbf{\Lambda}$ is the diagonalized $\mathbf{V}$. These two spins cannot control the contraction after unloading and extension following the contraction. On the other hand, when the plastic spin which is defined as a function of inelastic rate of deformation tensor and the Cauchy stress tensor, see Eq. (18) in Kuroda (1997), are used, the cyclic Swift effect has been reproduced successfully. It is pointed out that plastic spin associated with an anisotropic yield surface plays an important role in the simulation of the reverse shearing behavior.

In an other paper, Kuroda (1999) compared the predictions of the phenomenological model which is described in the aforementioned reference, Kuroda (1997), with the physically based crystal plasticity model which uses the Taylor assumption. It is shown that both models can predict the cyclic Swift effect quite well.

Majors and Krempl (1994) investigated the behavior of materials under free-end torsion using anisotropic VBO. Free-end torsion simulations performed using isotropic finite VBO, see Majors and Krempl (1994) and Majors (1993), revealed that only the monotonic Swift effect can be reproduced. It was pointed out that an anisotropic flow law was needed to model induced anisotropy. An anisotropic flow law is introduced into the VBO model by incorporating a fourth order inelastic compliance tensor into flow law. Only was the evolution of this tensor expressed for the special cases, which were simulated. It is shown that axial contraction after reversal of shear can be reproduced by anisotropic VBO.

Gomaa (1999) developed computational procedures for the finite element implementation of the finite deformation VBO for fixed and deformation induced anisotropy. State variables are defined in the Lagrangian rotated configuration. A hypoelastic relation between the Lagrangian logarithmic Cauchy stress rate and rotated rate of deformation is used. Simulation results show that backtracking can be reproduced, but unloading curve follows almost the loading curve.

Recently, a phenomenological model, which accounts for the evolution of the elastic and plastic properties due to the texture development, is developed by Boehlke et al. (2001). A hyper-elastic law between the Kirchhoff stress and the Almansi strain is used. The elastic stiffness tensor is decomposed into isotropic and anisotropic parts. The anisotropic part of the stiffness tensor is defined in terms of lattice vectors of the single crystals on the microscale. The viscoplastic flow law is assumed to be a function of an overstress and depends on the anisotropic part of the elasticity tensor. The model is applied to investigate the axial elongation, which develops during free-end torsion. In addition to the phenomenological model, a polycrystal model, the Taylor–Lin model, is used to model free-end torsion. The simulation results of the Taylor–Lin model and phenomenological model are compared. It is shown that although the phenomenological model can predict the monotonic and cyclic Swift effect quantitatively, the Taylor–Lin model over-predicts the axial elongation by a factor of 5.

In this paper, following Gomaa (1999), the finite deformation isotropic viscoplasticity theory based on overstress (FVBO) is extended to the anisotropic case. This is accomplished by formulating an anisotropic flow law, which consists of a fourth order inelastic compliance tensor. The aforementioned tensor used by Gomaa (1999) is modified. It is allowed to evolve according to a Frederick–Armstrong type growth law since inelastic deformation causes a change in the microstructure. Two tensor valued and one scalar valued state variable are defined in the Eulerian configuration.

5. Anisotropic VBO

Viscoplasticity theory based on overstress is a unified state variable theory with no yield surface and loading–unloading conditions (Krempl, 1996, 1998). Rate dependency, monotonic and cyclic loading, cyclic neutral behavior, creep, relaxation and kinematic hardening can be reproduced with this theory which consists of a maximum of four state variables with a flow law. The state variables are: the tensor valued equilibrium and kinematic stresses and a scalar valued isotropic and drag stress. The equilibrium stress is the stress that material can sustain when all rate s go to zero. It is related with defect structure of the material. tensor values kinematic stress is introduced to model kinematic hardening and set the tangent modulus at the maximum inelastic strain of interest. The scalar isotropic stress is the repository for cyclic hardening and softening (Krempl, 1998). The scalar drag stress is responsible for non-linear rate dependency. In this study, non-linear rate dependency is modeled by a viscosity function.

Following Chow (1993) and Gomaa (1999), the small deformation, isotropic VBO is extended to the finite deformation anisotropic case. The current configuration is taken as a reference configuration. Additive decomposition of the rate of deformation tensor, which is the symmetric part of velocity gradient tensor, is used. The rate of deformation tensor is the sum of the elastic and inelastic rate of deformation tensor.

A hypoelastic relation between the Eulerian Cauchy stress rate and elastic rate of deformation tensor is as follows:

$$\mathbf{D}^{\mathrm{e}} = \frac{D}{Dt}(\mathbb{S}\boldsymbol{\sigma}) \tag{4}$$

where $\mathbb{S}$ is the fourth order, symmetric elastic compliance tensor. D/Dt designates an objective time derivative. The objective Cauchy stress rates, $\overset{\circ}{\boldsymbol{\sigma}}$ is defined as

$$\overset{\circ}{\boldsymbol{\sigma}} = \dot{\boldsymbol{\sigma}} + \boldsymbol{\sigma}\boldsymbol{\Omega} - \boldsymbol{\Omega}\boldsymbol{\sigma} \tag{5}$$

where $\boldsymbol{\Omega}$ is a skew-symmetric spin tensor so that $\overset{\circ}{\boldsymbol{\sigma}}$ is objective.

The evolution equation of the equilibrium stress, $\mathbf{G}$, which is the stress that must be overcome to generate inelastic deformation is (Lee and Krempl, 1991),

$$\overset{\circ}{\mathbf{G}} = \frac{\Psi[\Gamma]}{E}\left(\overset{\circ}{\boldsymbol{\sigma}} + \frac{\boldsymbol{\sigma} - \mathbf{G}}{k[\Gamma]} - \frac{\Gamma}{k[\Gamma]}\left(\frac{\mathbf{G} - \mathbf{K}}{A + \beta\Gamma}\right)\right) + \left(1 - \frac{\Psi[\Gamma]}{E}\right)\overset{\circ}{\mathbf{K}} \tag{6}$$

The shape functions are limited by $0 \leqslant \Psi/E < 1$ and $\Psi > 0$. They can be function of overstress or can be constant. Elastic hardening is modeled when $\Psi \neq 0$. The quantity Ψ affects the transition from the quasi elastic to inelastic region. It is given by

$$\Psi[\Gamma] = C_1 + \frac{C_2 - C_1}{\exp(C_3\Gamma)} \tag{7}$$

$k[\Gamma]$ is decreasing positive viscosity function. It is responsible for modeling non-linear rate sensitivity and given by

$$k = k_1\left[1 + \frac{\Gamma}{k_2}\right]^{-k_3} \tag{8}$$

For modeling rate non-linear dependency, flow function can also be used. The relation between flow function, $F[\ ]$ and viscosity function, $k[\Gamma]$ is given as $F[\frac{\Gamma}{D}] = \frac{\Gamma}{Ek[\Gamma]}$ with D is the drag stress, which can be considered as another state variable.

The dimensionless factor β in Eq. (6) is set to zero for modeling positive rate sensitivity. Negative and zero rate sensitivities can be produced by setting $\boldsymbol{\beta} < -1$ and $\boldsymbol{\beta} = -1$, respectively (Ho and Krempl, 2000).

The first two terms in the evolution equation of the equilibrium stress are the elastic and inelastic hardening terms. The term having the negative sign is the dynamic recovery term. **K** is the kinematic stress, which is the repository for the Bauschinger effect.

The growth law for the kinematic stress is given as,

$$\overset{\circ}{\mathbf{K}} = \frac{E_{\mathrm{t}}}{k[\Gamma]}(\boldsymbol{\sigma} - \mathbf{G}) \tag{9}$$

where E_{t} is the tangent modulus at the maximum inelastic strain of interest.

The repository for modeling cyclic hardening and softening is the isotropic stress. Its evolution is given as

$$\dot{A} = A_c(A_f - A)\overline{D}^{\mathrm{in}} \tag{10}$$

where A_c and A_f material constants. For cyclic neutral behavior, the isotropic stress is constant ($A_c = 0$). If the initial value of the isotropic stress is less (higher) than the final values, cyclic hardening (softening) is modeled. $\overline{D}^{\mathrm{in}}$ is the effective inelastic rate of deformation,

$$\overline{D}^{\mathrm{in}} = \frac{\Gamma}{K_{\mathrm{o}}k[\Gamma/D]} = F\left[\frac{\Gamma}{D}\right] \tag{11}$$

where K_{o} is a constant with dimension of stress. Γ is the overstress invariant.

Most of the plasticity and viscoplasticity models that use a yield surface and isotropic and kinematic hardening variables account for deformation induced anisotropy by a von Mises type anisotropic yield criterion. In finite VBO, anisotropy will be induced by an anisotropic flow law given as:

$$\mathbf{D}^{\mathrm{in}} = \frac{\overline{D}^{\mathrm{in}}}{\Gamma}\mathbb{R} : \mathbf{O} \tag{12}$$

where $\mathbb{R}$ is an inelastic fourth order compliance tensor without dimension. **O** is the overstress, which is defined as the difference between the Cauchy and the equilibrium stresses. The overstress invariant is defined as

$$\Gamma = \sqrt{(\mathbb{R} : \mathbf{O}) : (\mathbb{R} : \mathbf{O})} \tag{13}$$

Since experiments show that the elastic and inelastic compliance can change during large deformation, the inelastic compliance tensor $\mathbb{R}$, is allowed to evolve at large strains. It is assumed that the elastic constants do not change due to large deformation. Frederick–Armstrong type law is used as a growth law for inelastic compliance tensor $\mathbb{R}$.

$$\overset{\circ}{\mathbb{R}} = \overline{D}^{\mathrm{in}}b[\bar{e}](\mathbb{R} - \mathbb{T}) \tag{14}$$

Objective rate of inelastic compliance tensor is given in component form by Sham (1999),

$$\overset{\circ}{\mathbb{R}}_{ijkl} = \dot{\mathbb{R}}_{ijkl} + \mathbb{R}_{mjkl}\boldsymbol{\Omega}_{mi} + \mathbb{R}_{imkl}\boldsymbol{\Omega}_{mj} + \mathbb{R}_{ijml}\boldsymbol{\Omega}_{mk} + \mathbb{R}_{ijkm}\boldsymbol{\Omega}_{ml} \tag{15}$$

$\mathbb{T}$ is the symmetric texture compliance tensor given by

$$\mathbb{T} = (\mathbb{R}_{\mathrm{o}} : \boldsymbol{\chi}) \otimes (\mathbb{R}_{\mathrm{o}} : \boldsymbol{\chi}) \tag{16}$$

The texture compliance tensor is comprised of the initial inelastic compliance tensor $\mathbb{R}_o$ and the direction of inelastic rate of deformation tensor, $\boldsymbol{\chi}$. This tensor combines the compliance obtained from a prior history with the present direction of inelastic straining. The direction of inelastic rate of deformation tensor, $\boldsymbol{\chi}$ is given by

$$\boldsymbol{\chi} = \frac{1}{\Gamma}\mathbb{R} : \mathbf{O} \tag{17}$$

The rate of growth of the inelastic compliance is controlled by the dimensionless positive function $b[\bar{e}]$. During inelastic deformation, the reorientation of grains along preferred directions is observed. The most types of deformation do not produce a single orientation but rather a range of orientations (Rollett and Wright, 1998). Experiments have shown that "individual orientations may rotate quickly into the range of characteristic orientations, then rotate slowly within that range" (Rollett and Wright, 1998). Therefore, the function $b[\bar{e}]$ is chosen as a decreasing function to simulate the decreasing rate of orientational changes. $b[\bar{e}]$ function is defined as a function of accumulated inelastic strain $\bar{e}$ given by

$$\bar{e}(t) = \int \overline{D}^{\text{in}}(\tau)\,\mathrm{d}\tau \tag{18}$$

6. Conclusions

The isotropic finite viscoplasticity theory based on overstress, which is a unified state variable theory is extended to anisotropy. An anisotropic fourth order inelastic compliance tensor is introduced into the flow law. During large deformation, initially isotropic material can become anisotropic. Therefore, the inelastic compliance tensor is allowed to evolve during large inelastic deformation. Two tensor valued and a scalar state variables are defined at the Eulerian frame.

A hypoelastic relation between the objective rate of Cauchy stress and the elastic part of the rate of deformation tensor is assumed. The inelastic part of the rate of deformation tensor is function of the overstress, the difference between the Cauchy stress and the equilibrium stress through a fourth order inelastic compliance tensor.

References

Asaro, R.J., Needleman, A., 1985. Texture development and strain hardening in rate dependent polycrystals. Acta Metallurgica 33 (6), 923–953.

Bertram, A., Bohlke, T., Kraska, M., 1997. Numerical simulation of deformation induced anisotropy of polycrystals. Computational Materials and Science 9, 158–167.

Billington, E.W., 1976. Non-linear mechanical response of various metals: II. Permanent length changes in twisted tubes. Journal of Physics D: Applied Physics 9, 533–552.

Billington, E.W., 1977a. Non-linear mechanical response of various metals: I. Dynamic and static response to simple compression, tension and torsion in the as-received and annealed states. Journal of Physics D: Applied Physics 10, 519–531.

Billington, E.W., 1977b. Non-linear mechanical response of various metals: III. Swift effect considered in relation to stress–strain behavior in simple compression, tension and torsion in the as-received and annealed states. Journal of Physics D: Applied Physics 10, 553–569.

Boehlke, T., Bertram, A., Krempl, E., 2001. Modeling of deformation induced anisotropy. Society for Engineering Science Meeting, San Diego, CA.

Chow, H., 1993. A finite element method for an incremental viscoplasticity theory based on overstress. Ph.D. Thesis. Rensselaer Polytechnic Institute, Troy, New York.

Dafalias, Y.F., 1990. The plastic spin in viscoplasticity. International Journal of Solids and Structures 26 (2), 149–163.

Gomaa, S., 1999. Computational procedures for finite deformation rate-independent plasticity and visco-plasticity based on overstress. PhD. Thesis. Rensselaer Polytechnic Institute, Troy, New York.

Harren, S., Lowe, T.C., Asaro, R.J., Needleman, A., 1989. Analysis of large strain shear in rate dependent face centered cubic polycrystals: correlation of micro and macromechanics. Philosophical Transactions of the Royal Society of London, Series A 328, 443–500.

Hill, R., 1953. Theory of yielding and plastic flow of anisotropic metals. Proceedings of the Royal Society of London, Series A 193, 281.

Ho, K., Krempl, E., 2000. Modeling of positive, negative and zero rate sensitivity by using the viscoplasticity theory based on overstress (VBO). Mechanics of Time Dependent Materials 4, 21–42.

Khan, A., Cheng, P., 1998. An anisotropic elastic–plastic constitutive model for single and polycrystalline metals. II. Experiments and predictions concerning thin-walled tubular OFHC copper. International Journal of Plasticity 14 (1–3), 209–226.

Krempl, E., 1994. Deformation induced anisotropy. Rensselaer Polytechnic Institute Report. Mechanics of Materials Laboratory. 94-3.

Krempl, E., 1996. A small strain viscoplasticity theory based on overstress. In: Krausz, A.S., Krausz, K. (Eds.), Unified Constitutive Laws of Plastic Deformation. Academic Press, San Diego. pp. 281–318.

Krempl, E., 1998. Creep-plasticity interaction. Lecture notes. CISM No: 187. Udine, Italy. 74.

Kuroda, M., 1997. Interpretation of the behavior of metals under large plastic shear deformations: a macroscopic approach. International Journal of Plasticity 13 (4), 359–383.

Kuroda, M., 1999. Interpretation of the behavior of metals under large plastic shear deformations: comparison of macroscopic predictions to physically based predictions. International Journal of Plasticity 15, 1217–1236.

Lee, D., 1978. A continuum description of anomalous yielding in anisotropic metals. Metallurgical Transactions A 9A, 1495–1497.

Lee, D., Zaverl, F., 1978. A generalized strain rate dependent constitutive equation for anisotropic metals. Acta Metallurgica 26, 1771–1780.

Lee, D., Zaverl, F., 1979. A description of history dependent plastic flow behavior of anisotropic metals. Journal of Engineering Materials and Technology 101, 59–67.

Lee, K.-D., Krempl, E., 1991. An orthotropic theory of viscoplasticity theory based on overstress for thermomechanical deformations. International Journal of Solids and Structures 27, 1445–1459.

Lehmann, T., 1990. Some considerations concerning deformation induced anisotropy. In: Yielding, Damage, and Failure of Anisotropic Solids. EGFS, Mechanical Engineering Publications. pp. 83–96.

Loret, B., 1983. On the effects of plastic rotation in the finite deformation of anisotropic elastoplastic materials. Mechanics of Materials 2, 287.

Lowe, T.C., Lipkin, J., 1991. Analysis of axial deformation response during reverse shear. Journal of Mechanics and Physics of Solids 39 (3), 417–440.

Majors, P., 1993. Modeling of rate dependent deformation of metals and alloys using the viscoplasticity theory based on overstress: behavior of modified 9Cr-1Mo steel at 538 degrees Celsius and deformation induced anisotropy at finite strains. Ph.D. Thesis. Rensselaer Polytechnic Institute, Troy, New York.

Majors, P., Krempl, E., 1994. Comments on induced anisotropy, the Swift effect, and finite deformation inelasticity. Mechanics Research Communications 21, 465–472.

Montheillet, F., Cohen, M., Jonas, J.J., 1984. Axial stresses and texture development during the torsion testing of Al, Cu, and α-iron. Acta Metallurgica 32 (11), 2077–2089.

Montheillet, F., Gilormini, P., Jonas, J.J., 1985. Relation between axial stresses and texture development during torsion testing: A simplified theory. Acta Metallurgica 33 (4), 705–707.

Mroz, Z., Niemunis, A., 1990. On the description of deformation anisotropy of materials. In: Yielding, Damage and Failure of Anisotropic Solids. EGFS5, Mechanical Engineering Publications, London. pp. 171–186.

Neale, K.W., Toth, L.S., Jonas, J.J., 1990. Large strain shear and torsion of rate-sensitive FCC polycrystals. International Journal of Plasticity 6, 45–61.

Nouailhas, D., Chaboche, J.L., 1991. Anisotropic constitutive modeling for single crystal superalloys using a continuum phenomenological approach. Third International Conference on Constitutive Laws for Engineering Materials, Theory and Applications. Arizona.

Rollett, A.D., Wright, S.I., 1998. Typical textures in metals. In: Kocks, U.F., Tome, C.N., Wenk, H.R. (Eds.), Texture and Anisotropy. Cambridge University Press.

Sham, T.L., 1999. Objective rate of fourth order Eulerian tensor. Personal communication.

Shih, C.F., Lee, D., 1978. Further developments in anisotropic plasticity. Transactions of the ASME 100, 294–302.

Stouffer, D., Dame, T., 1996. Inelastic Deformation of Metals. Wiley, New York.

Swift, H., 1947. Length changes in metals under torsional overstrain. Engineering 163, 253–257.

Taylor, G.I., 1938. Plastic strain in metals. Journal of Institute of Metals 62, 307–324.

Van der Giessen, E., Wu, P.D., Neale, K.W., 1992. On the effect of plastic spin on large strain elastic-plastic torsion of solid bars. International Journal of Plasticity 8, 773–801.

Voyiadjis, G., Kattan, P., 1992. Finite elasto-plastic analysis of torsion problems using different spin tensors. International Journal of Plasticity 8, 271–314.

Wu, P.D., Neale, K.W., Van der Giessen, E., 1996. Simulation of the behavior of FCC polycrystals during reversed torsion. International Journal of Plasticity 12 (9), 1199–1219.

Wu, H., Xu, Z., Wang, P., 1998. Torsion test of aluminum in the large strain range. International Journal of Plasticity 13 (10), 873–892.